ELECTRONIC SUPPLEMENTARY INFORMATION

Attomolar protein detection using a magnetic bead surface coverage assay

H. Cumhur Tekin, Matteo Cornaglia and Martin A. M. Gijs*

Laboratory of Microsystems, Ecole Polytechnique Fédérale de Lausanne (EPFL), CH-1015, Lausanne, Switzerland.

*To whom correspondence should be addressed.
E-mail: martin.gijs@epfl.ch, tel: +41 21 693 77 31, fax : +41 21 693 59 50

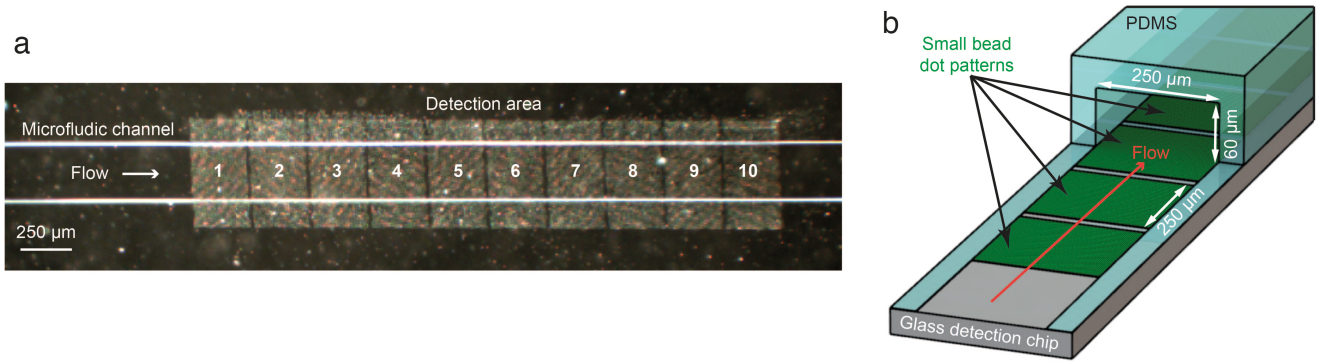

Fig. S1 (a, b) Optical microscopy photograph and schematic representation of the detection area, respectively. For ease of visualization of bound large beads, the detection area is fabricated as ten sections composed of small bead dot patterns, each covering a 250 µm × 250 µm area at the bottom of a microfluidic channel.

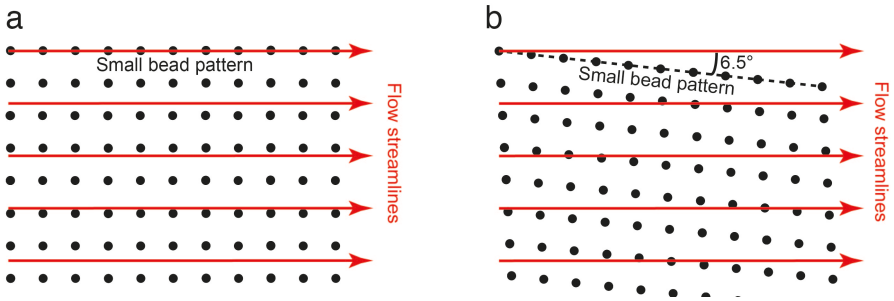

Fig. S2 Flow streamline profile on (a) non-tilted and (b) 6.5° tilted small bead patterns. In absence of magnetic dipolar forces, the large beads would be carried along these streamlines over the patterns and clearly would more efficiently expose the small bead pattern in the case (b).

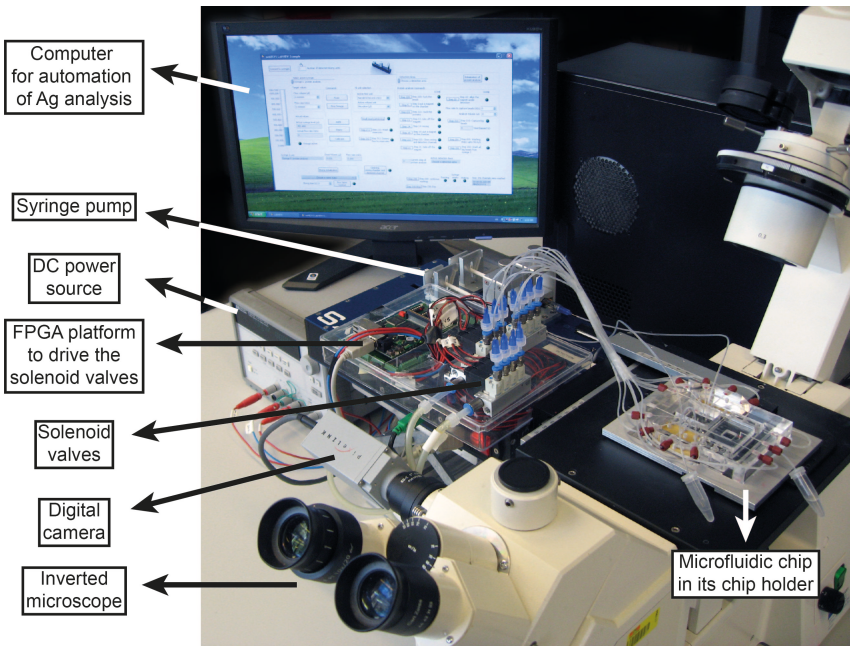

Fig. S3 Photograph of the experimental setup with the microfluidic PDMS chip placed in its holder.

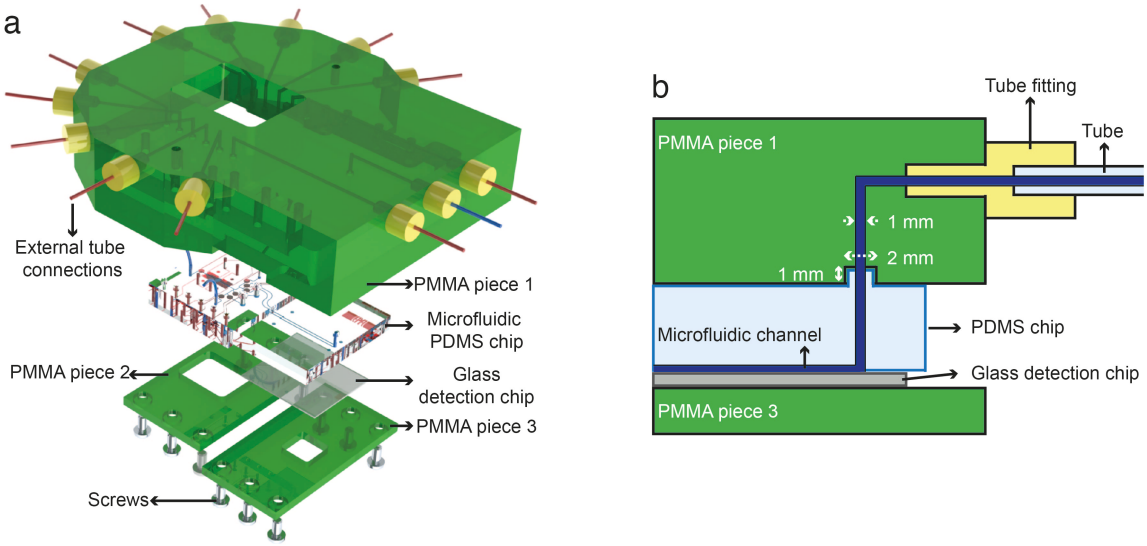

Fig. S4 Microfluidic chip holder made from polymethylmethacrylate (PMMA). (a, b) A schematic view and a partial cross-section view of the disassembled and assembled microfluidic chip holder, respectively. The microfluidic PDMS chip and the glass detection chip are clamped between PMMA pieces with screws. PMMA piece 1 also provides the interface between the external tubes and the microfluidic chip.

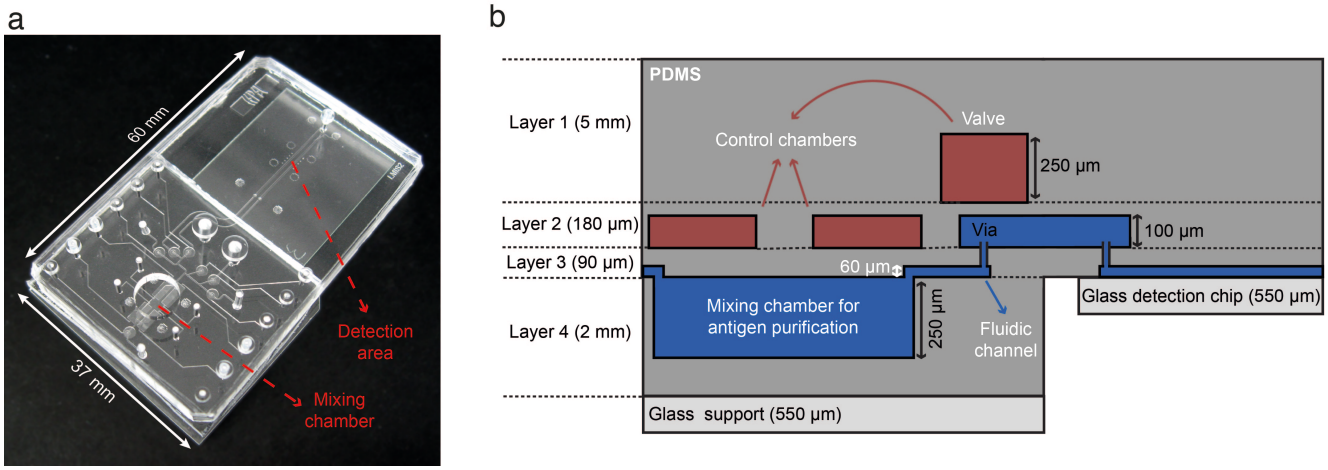

Fig. S5 Microfluidic chip. (a) Photograph of a microfluidic chip containing a 5 µL mixing chamber and detection area for on-chip antigen analysis. (b) Cross-sectional view of the microfluidic chip composed of four PDMS layers. 80-90 µm thick PDMS membranes are realized between control and fluidic layers. For valving, the thin membrane is actuated by pressurizing the valve control chamber closing the microfluidic via. For antigen purification, active mixing is obtained by inducing source-sink flows in the mixing chamber by pressurizing one mixing control chamber (source) while releasing pressure in a neighboring one (sink). Geometrical parameters of the PDMS layers are given on the figure and detailed information on valving and mixing functionalities can be found elsewhere[1].

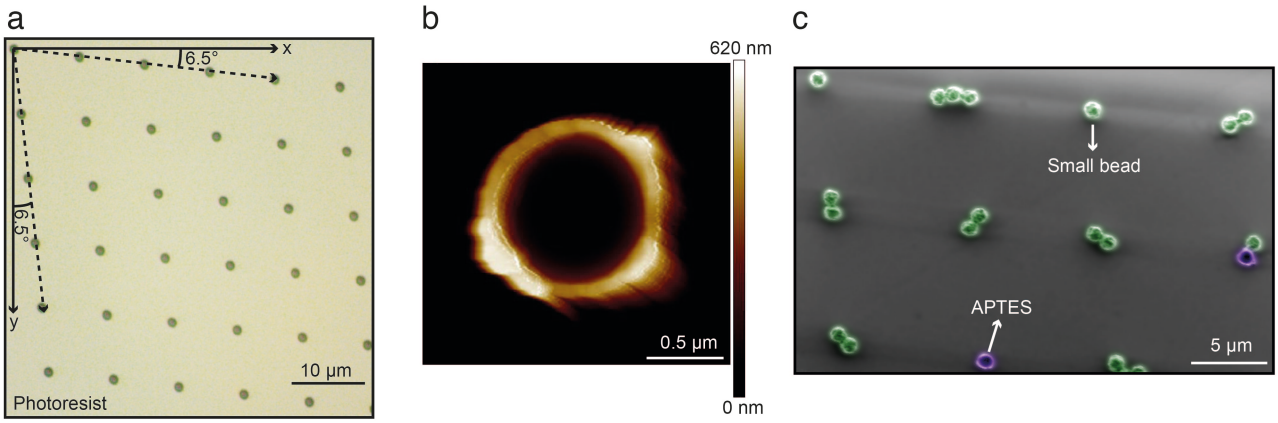

Fig. S6 Realization of the glass detection chip. (a) Optical microscopy photograph of a detection chip covered with 0.6 µm thick AZ ECI 1512 positive photoresist structures used for realizing the APTES dot patterns. The dots are obtained by first spin-coating of the APTES layer on the photoresist patterns, after which the photoresist is removed in an acetone bath in a lift-off-type process. (b) AFM image of a 1.5 µm APTES dot after the photoresist lift-off process. The scale on the right represents the height of the APTES pattern. (c) SEM photograph of a part of the detection area after small bead patterning. The image is artificially colored to emphasize the small beads and APTES patterns.

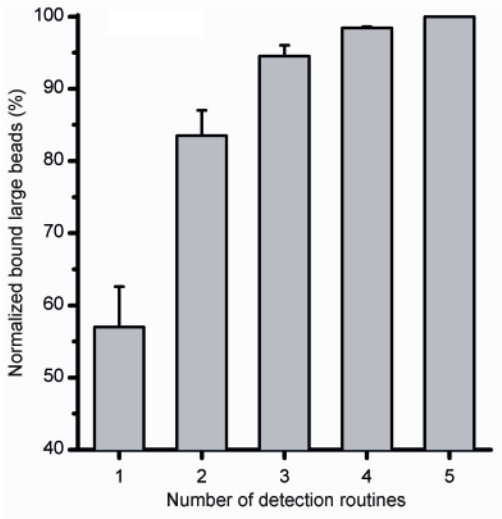

Fig. S7 Analysis of 10 µg/mL biotinylated anti-streptavidin in PBS using a different number of detection routines. A detection routine is defined in the "Microfluidic protocol for protein analysis" part of the Experimental. Normalization is performed by dividing by the total number of beads counted after five detection routines. It is seen that, after conducting 3 detection routines, we can transfer 95 % (SD 2 %) of the large beads from the mixing chamber to the detection area. Error bars represent means ± SD over 3 replicates.

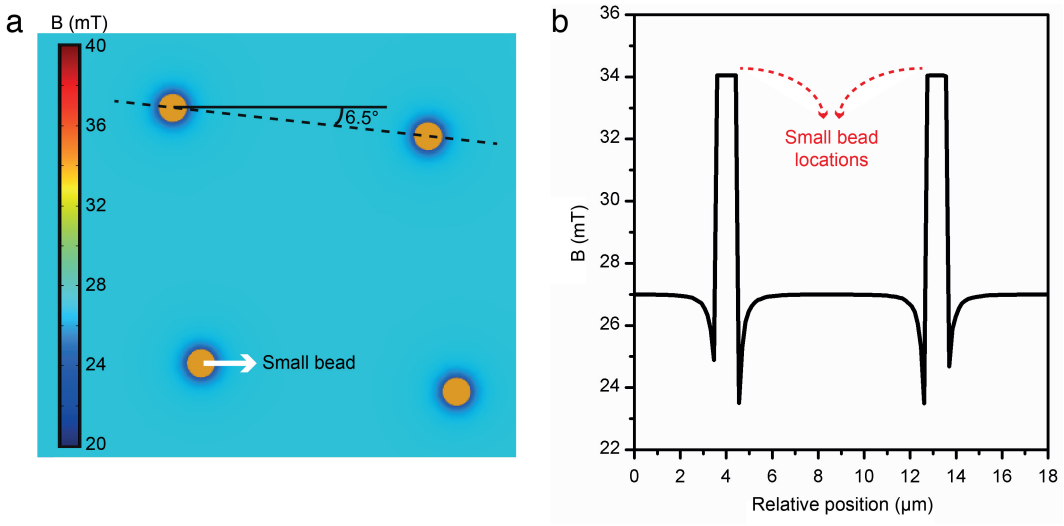

Fig. S8 Magnetic induction profile (**B**) on the detection area. (a) **B** profile obtained from FEM simulations on the glass detection chip in the presence of a 6.5° tilted small bead pattern. (b) Slice plot passing through the centers of small beads showing the local **B** profile along the dashed-line presented in (a).

Movie S1 Slow-motion video clip, as recorded by a high-speed camera, of the transportation of large magnetic beads over surface-immobilized small magnetic beads using a 100 nL/s flow rate under application of a 27 mT magnetic field. Small beads are streptavidin-coated and large beads either do not carry antigens and interact with the small beads only via magnetic dipole interactions (first part of the movie), or carry antigens (biotinylated anti-streptavidin) and bind to the small beads (second part of the movie). In the latter case, large beads, having captured antigens, were subsequently incubated with streptavidin-coated non-magnetic beads (0.5 μm diameter; acquired from Bang Laboratories, Fishers, IN, USA), to form a small cluster that allows better visualization of the beads' trajectory. The movie clearly shows how large beads adhere temporarily to the small beads due to the magnetic dipole-dipole forces and roll over them due to the combination of magnetic and drag forces.

Table S1 Magnetic dipolar forces between a large bead and a pattern of a few small beads. The magnetic forces are calculated for a 27 mT magnetic induction using the magnetic bead properties[2, 3].

Number of small beads on an APTES dot with 1.5 μm diameter	Maximum dipolar magnetic force induced on a large bead (pN)
1	20
2	30
4	45

Table S2 Comparison of today's most sensitive antibody-based methods for rare protein detection in serum. The detection methods are ranked with respect to their LOD.

Detection method	Target antigen*	LOD in whole serum† (g/mL)	Sample volume (V_S) (μL)	Number of molecules (NM) in whole serum‡	Sample capture time (min)	Total assay time (T_A) (min)	Figure of merit§ (FM)
Commercially available ELISA[4]	TNF-α	3×10^{-13}	200	3×10^{6}	180	>360	1×10^{0}
Bio-barcode[5]	PSA	3×10^{-13}	30	2×10^{5}	60	> 210	3×10^{1}
Magnetic bead surface coverage assay[6]	SEB	1×10^{-13}	1000	2×10^{6}	5	20	2×10^{1}
Fluorescent confocal microscopy[7]	TNF-α	2×10^{-14}	200	2×10^{5}	120	>180	4×10^{1}
Digital ELISA[4]	TNF-α	1×10^{-14}	100	4×10^{4}	120	360	7×10^{1}
Magnetic bead surface coverage assay[8]	PSA	1×10^{-14}	40	7×10^{3}	90	100	1×10^{3}
PCR coupled bio-barcode[9]	PSA	1×10^{-15}	10	2×10^{2}	30	> 240	2×10^{4}
Our method	**TNF-α**	**1×10^{-15}**	**5**	**2×10^{2}**	**1**	**20**	**2×10^{5}**

* Abbreviations of target antigens: Tumor Necrosis Factor-α (TNF-α), Prostate Specific Antigen (PSA), and Staphylococcal Enterotoxin B (SEB).
† Some of the detection methods work only in diluted serum. Their detection limits are converted to whole (100 %) serum conditions.
‡ NM = LOD × V_S × N_A / MW, where LOD is in whole serum, N_A is the Avogadro number and MW is the molecular weight of the target antigen. LOD is calculated as background plus 3 SD in references 4, 5 and 8, and as 2 SD of the signal from the background divided by the slope of the linear portion of the detected event signal in reference 7. The calculation of LOD is not explicitly mentioned in references 6 and 9.
§ FM = 1/ (NM × T_A). FM values presented in the table are normalized by the ELISA data.

References

1 H. C. Tekin, V. Sivagnanam, A. T. Ciftlik, A. Sayah, C. Vandevyver and M. A. M. Gijs, *Microfluid. Nanofluid.*, 2011, **10**, 749-759.
2 G. Fonnum, C. Johansson, A. Molteberg, S. Morup and E. Aksnes, *J. Magn. Magn. Mater.*, 2005, **293**, 41-47.
3 K. C. Neuman, T. Lionnet and J. F. Allemand, *Annu Rev Mater Res*, 2007, **37**, 33-67.
4 D. M. Rissin, C. W. Kan, T. G. Campbell, S. C. Howes, D. R. Fournier, L. Song, T. Piech, P. P. Patel, L. Chang, A. J. Rivnak, E. P. Ferrell, J. D. Randall, G. K. Provuncher, D. R. Walt and D. C. Duffy, *Nat. Biotechnol.*, 2010, **28**, 595–599.
5 C. S. Thaxton, R. Elghanian, A. D. Thomas, S. I. Stoeva, J. S. Lee, N. D. Smith, A. J. Schaeffer, H. Klocker, W. Horninger, G. Bartsch and C. A. Mirkin, *P. Natl. Acad. Sci. USA*, 2009, **106**, 18437-18442.
6 S. P. Mulvaney, K. M. Myers, P. E. Sheehan and L. J. Whitman, *Biosens. Bioelectron.*, 2009, **24**, 1109-1115.
7 J. Todd, B. Freese, A. Lu, D. Held, J. Morey, R. Livingston and P. Goix, *Clin Chem*, 2007, **53**, 1990-1995.
8 S. Krishnan, V. Mani, D. Wasalathanthri, C. V. Kumar and J. F. Rusling, *Angew. Chem. Int. Ed.*, 2011, **50**, 1175-1178.
9 J. M. Nam, C. S. Thaxton and C. A. Mirkin, *Science*, 2003, **301**, 1884-1886.